


Cite this: *Anal. Methods*, 2018, 10, 308

## Chemistry of extracting high-contrast invisible fingerprints from transparent and colored substrates using a novel phosphorescent label†

G. Swati,<sup>ab</sup> Swati Bishnoi,<sup>ab</sup> Paramjeet Singh,<sup>ab</sup> Naina Lohia,<sup>ab</sup> Vishnu V. Jaiswal,<sup>a</sup> M. K. Dalai<sup>ab</sup> and D. Haranath<sup>ab</sup> 

Traditionally used fluorescent powders for developing invisible (latent) fingerprints involve complicated operation and show characteristics of auto-fluorescence interference and high toxicity. To overcome these serious drawbacks we report a novel application and facile methodology to extract high contrast fingerprints on non-porous and porous substrates using a chemically inert, visible light excitable, and nanosized SrAl<sub>2</sub>O<sub>4</sub>:Eu<sup>2+</sup>, Dy<sup>3+</sup> phosphorescent label in the dark. The chemistry of non-covalent physisorption interaction between the long afterglow phosphor powder and sweat residue in fingerprints has been discussed in detail. Real-time fingerprint development on porous and non-porous substrates has also been performed.

Received 24th November 2017  
Accepted 25th November 2017

DOI: 10.1039/c7ay02713c

rsc.li/methods

Every fingertip has a distinct and characteristic ridge and furrow pattern, with no two fingertips sharing an identical arrangement. Fingerprints as-obtained from a crime scene can be in the form of patent, plastic and latent prints. Visible prints are left on substrates after ridges on volar pads come into contact with substances such as paint, ink or blood that render the prints clearly visible. Plastic prints are left on soft surfaces, such as clay or wet paint. Latent prints are print impressions caused by perspiration. These are invisible and need to be developed *via* physical or chemical processing. Various physical and chemical treatments to study latent fingerprints have been developed. These include powder dusting, vacuum metal deposition, ninhydrin, cyanoacrylate, and iodine fuming, and fluorescence staining.<sup>1,2</sup> Of all these treatments, powder dusting is an extremely facile and effective method to develop latent fingerprints.<sup>3,4</sup> Latent fingerprints are developed by dusting off the substrate area with suitable powder, causing particulates of the fuming powder to adhere mechanically, physically or chemically to the residue left by friction ridge skin on fingers, papillary ridges, palms, and feet. The residue of the fingerprint surface comprises organic material, such as amino acids, proteins, moisture, lipids, creatinine, choline, and lactic acid.<sup>5</sup> Selection of the dusting powder is a critical step dictating the color contrast in developed fingerprints. Conventionally black

colored fine carbon powder is used for dusting light colored substrates, and off-white colored fine alumina dust is used on metallic and dark colored substrates.<sup>6</sup> However, in the case of colored and transparent substrates, it is difficult to visualize high contrast latent fingerprint patterns, which can cause loss of valuable information during the crime scene investigation process.

In the recent past, fluorescent dyes (such as rhodamine, azure, Congo-red, and eosin yellow)<sup>7</sup> and quantum dots (TiO<sub>2</sub>, CdSe, CdS, and ZnS)<sup>8–10</sup> have been used for lifting fingerprints on a colored substrate. Near-infrared emitting up-conversion (NaYF<sub>4</sub>:Yb,Er/Ce) phosphors<sup>11–13</sup> have also been used to enhance the contrast of the developed fingerprints. However rapid visualisation of latent fingerprints, directly at the crime scene, is difficult due to the requirement of selective light sources such as laser excitation. Table 1 lists the types of luminescent powders with their merits and demerits for developing latent fingerprints. Apart from luminescent powders, time resolved photoluminescence is an effective way to resolve weak and low contrast fingerprints. In this method the short-lived fluorescence from the background is chopped off from the longer-lived fingerprint luminescence. However, this method uses sophisticated optical grating instruments. Traditionally utilised materials also have serious drawbacks. Firstly they require a source of continuous excitation emitting in the short ultraviolet (UV) or near infrared region; secondly, most of the substrates such as paper, polyethylene, textile and other organic based materials show auto-fluorescence under UV (375 nm) light resulting in a low signal to noise ratio. Moreover, the carcinogenic nature of these materials presents potential health hazards to persons involved in forensic and medical sciences.

<sup>a</sup>CSIR – National Physical Laboratory, Dr K S Krishnan Road, New Delhi-110 012, India. E-mail: haranath@nplindia.org

<sup>b</sup>Academy of Scientific and Innovative Research (AcSIR), CSIR-NPL Campus, New Delhi-110012, India

† Electronic supplementary information (ESI) available: TEM images and fluorescence confocal images of the as-prepared nanophosphor and its preparation. See DOI: 10.1039/c7ay02713c

**Table 1** Luminescent powders used for developing latent (invisible) fingerprints with their merits and demerits

Luminescent labels	Materials	Merits	Demerits
Organic fluorescent dyes	Rhodamine B dye, eosin yellow dye, eosin blue dye, Gunea green dye, aniline blue dye, cyno blue dye, azure dye, Congo red dye, and 1,8-diazafluoren-9-one	Results in fluorescent print which can be distinguished from a colored and/or printed background	(1) Requires a continuous source of excitation, (2) auto-fluorescence from the background can't be avoided, and (3) shows photobleaching
Fluorescent inorganic phosphors	CdSe, CdS, (PVP)-coated silica NPs, SiO <sub>2</sub> :Eu <sup>3+</sup> , CdS/dendrimer, carbon dots, ZnO:Li, and TiO <sub>2</sub>	Photochemically and thermally stable and high fluorescence intensity	(1) Requires a continuous source of excitation and (2) auto-fluorescence from the background can't be avoided
Up-conversion phosphors	NaYF <sub>4</sub> :Yb,Er, Sb <sub>2</sub> O <sub>3</sub> -WO <sup>3-</sup> , Li <sub>2</sub> O:Yb <sup>3+</sup> /Er <sup>3+</sup> , La <sub>2</sub> O <sub>3</sub> :Er <sup>3+</sup> /Yb <sup>3+</sup> , and NaGdF <sub>4</sub> Er <sup>3+</sup> /Yb <sup>3+</sup>	Background interference is negligible	Requires sophisticated lasers as the excitation source

The above-mentioned issues can be eliminated by using Long Afterglow (LA) phosphors to rapidly visualise high contrast fingerprints without any background interference.

LA phosphors represent a unique class of photon energy storage materials.<sup>14,15</sup> These can be readily excited by ambient white lighting, cold fluorescent lamps and even sunlight. Additionally, these have excellent piezoelectric properties and chemical as well as thermal stability with high quantum efficiency which broadens their potential applications in the fields of luminescent paints, photovoltaic devices, sensors for structural damage, photocatalysis under dark conditions, biological staining, and photodynamic therapy treatment for cancer.<sup>16-19</sup> Excitation by white light easily avoids auto-fluorescence from the substrate, thus enhancing the overall contrast of the latent fingerprints developed as compared to the results produced by using regular dusting powders. LA phosphor powders can be directly applied to the crime scene because they are readily excited by ambient lighting and do not need sophisticated instrumentation. Being chemically inert, they do not form chemical complexes with the substrate surface on which latent fingerprints are present. Fingerprints developed using LA phosphor powder can be easily lifted using clear tape and preserved. LA phosphor powder, being a stable inorganic material, does not show any photo or thermal bleaching effects. Thus fingerprints developed using LA phosphor powder can be stored for a longer period than those using fluorescent dyes. Unfortunately, despite having numerous benefits, LA phosphors have not been extensively explored for developing latent fingerprints, especially those on colored and transparent substrates, which are difficult to analyze using conventional powders. Only a handful of reports are available on investigations on the potential application of LA materials in the field of forensic science.<sup>20-22</sup> As a case study, we report the facile synthesis and efficient use of SrAl<sub>2</sub>O<sub>4</sub>:Eu<sup>2+</sup>,Dy<sup>3+</sup> phosphor powder for developing high contrast latent fingerprints from multi-colored and transparent polyethylene terephthalate (PET) substrates and the possible chemistry involved.

SrAl<sub>2</sub>O<sub>4</sub>:Eu<sup>2+</sup>,Dy<sup>3+</sup> phosphor powder was synthesized using a facile and self-propelling urea-combustion synthesis method followed by post-annealing in a reducing atmosphere of NH<sub>3</sub>-

N<sub>2</sub> as described in detail in our previous work<sup>23</sup> and in the ESI.† During the course of the reaction, urea plays a dual role as a fuel for combustion (high negative heat of combustion) and precipitating agent. Fresh fingermarks were collected from a healthy donor aged 26 years. The required ethical statement is included at the end of the research article. The fingermarks were deposited on non-porous and porous surfaces. The prepared powder was then applied to these surfaces using a squirrel hair brush. The developed fingermarks were then excited under UV (375 nm) and visible light. The developed fingerprints were stored in evidence bags after capturing photographs.

Fig. 1(a and b) show the powder-XRD profile of the as-synthesized SrAl<sub>2</sub>O<sub>4</sub>:Eu<sup>2+</sup>,Dy<sup>3+</sup> long afterglow phosphor sample, and the corresponding JCPDS card 034-0379 respectively. All the peaks were in good agreement with standard JCPDS data. The XRD profile of the sample corresponds to the monoclinic phase of SrAl<sub>2</sub>O<sub>4</sub>:Eu<sup>2+</sup>,Dy<sup>3+</sup> crystallized in a distorted stuffed tridymite structure. The monoclinic phase of SrAl<sub>2</sub>O<sub>4</sub> has a higher luminescence quantum efficiency<sup>24</sup> as a host matrix for Eu<sup>2+</sup> ions as compared to the hexagonal phase of SrAl<sub>2</sub>O<sub>4</sub>. Post-annealing

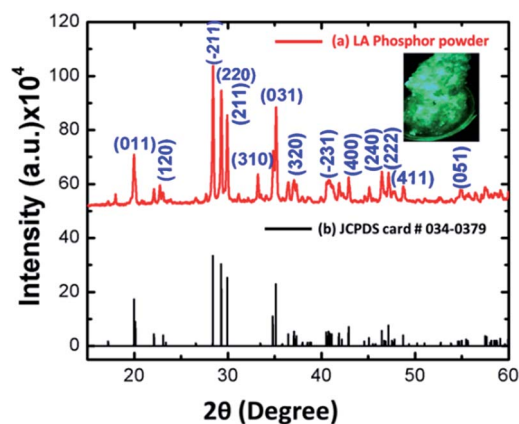


**Fig. 1** (a) Powder-XRD profile of the as-synthesized SrAl<sub>2</sub>O<sub>4</sub>:Eu<sup>2+</sup>,Dy<sup>3+</sup> long afterglow phosphor, and (b) standard JCPDS card 034-0379. The inset shows afterglow luminescence from the sample in the dark after excitation with white light for 5 minutes.

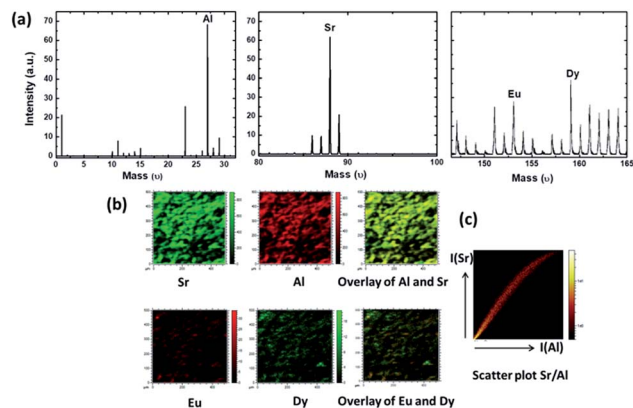


Fig. 2 (a) Selected range of positive SIMS spectra of  $\text{SrAl}_2\text{O}_4\text{:Eu}^{2+},\text{Dy}^{3+}$ , (b) TOF-SIMS chemical images of constituent elements and their two-colour overlay images and (c) 2D correlation analysis using a scatter plot for the distribution of Sr and Al.

treatment suppresses the formation of the hexagonal phase of  $\text{SrAl}_2\text{O}_4$ .  $\text{Eu}^{2+}$  (1.09 Å) ions are expected to substitute  $\text{Sr}^{2+}$  (1.12 Å) sites due to their similar ionic radii and formal charge. Bright field transmission electron microscopy images and the confocal fluorescence image of the as-prepared  $\text{SrAl}_2\text{O}_4\text{:Eu}^{2+},\text{Dy}^{3+}$  phosphor and their detailed discussion are given in the ESI.†

For analyzing the homogeneity of dopant distribution in the as-synthesized long afterglow phosphor, the TOF-SIMS chemical imaging technique was employed, and correlation analysis was done by using color overlay and scatter plot techniques. A  $500\ \mu\text{m} \times 500\ \mu\text{m}$  area of the sample has been considered and assigned different colors for Sr, Al, Eu and Dy ions. Fig. 2(a) presents the mass spectra in the positive polarity mode where the peaks of  $^{27}\text{Al}$ ,  $^{88}\text{Sr}$ ,  $^{153}\text{Eu}$  and  $^{164}\text{Dy}$  isotopes can be clearly seen. Low lying peaks at  $\text{amu} = 88$  are attributed to  $\text{Sr}^+$  ions. The mass spectra confirm the presence of Eu and Dy dopants in the phosphor material. Isotopes of Eu and Dy, *i.e.* ( $^{151}\text{Eu}$  and  $^{153}\text{Eu}$ ) and ( $^{160}\text{Dy}$ ,  $^{161}\text{Dy}$ , and  $^{162}\text{Dy}$ ) can also be detected. Peaks at  $\text{amu} = 12$  and  $15.9$  are attributed to the distribution of carbon and oxygen ions on the surface of the sample.

Fig. 2(b) shows the distribution of positive secondary ion images of strontium, aluminum, europium, and dysprosium. The intensity of the pixels correlates with the intensity of the mass signal in the color overlay images. The color overlay between  $^{153}\text{Eu}$  and  $^{164}\text{Dy}$  shows that both dopants are present simultaneously. However, the concentration of Dy exceeds that of Eu which is consistent with the initial dopant concentration selected for the experiment. The color overlay does not show homogeneity and there are scattered patches of dopants in some parts. As seen from Fig. 2(c), the scatter plot for Al and Sr (the main elemental constituents) shows good agreement close to  $45^\circ$  and is biased slightly towards the X-axis which indicates excess aluminum concentration.

The scheme adapted for developing latent fingerprints from substrates is presented in Fig. 3. Friction ridges have very minute pores (1–50  $\mu\text{m}$ ), which are the openings of sweat gland ducts. Sweat glands have a high concentration on the palms. The primary constituent of latent fingerprints is sweat, which

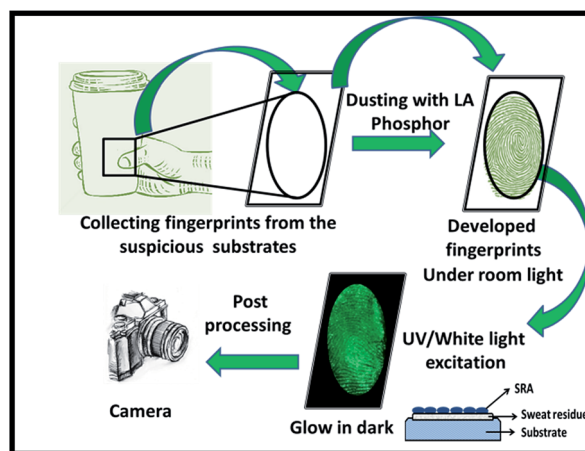


Fig. 3 Detailed scheme adapted for developing latent fingerprints using the  $\text{SrAl}_2\text{O}_4\text{:Eu}^{2+},\text{Dy}^{3+}$  long afterglow phosphor powder.

originates from three different types of glands: eccrine, apocrine and sebaceous glands. The detailed composition of the natural secretions from these glands is shown in Table 2.

The deposited fingerprints mostly contain moisture due to sweat (99%), fatty acids, lipids, alkaline salts, amino acids and other organic compounds. Hence, the particulates of the dusting powder adhere physically to these residues at the site of the fingerprints. More precisely, dusting of the fingerprints with powder is based on the pressure deficit in sweat droplets in which particulates of the fuming powder adhere to residues left behind by friction ridges on fingers, only on the lower side of sweat deposits due to which the curvature of the meniscus is formed which leads to pressure deficit, causing the particles to adhere to sweat droplets.<sup>26</sup>

Within a sweat droplet, all molecules move freely by virtue of their chemical potential. When phosphor powder is dusted, it dissolves in the sweat residue. Thus there is considerable loss of freely moving sweat molecules, which results in pressure deficit inside the droplet. In other words there is an increase in suction pressure in sweat droplets when dusted with phosphor powder over its pure phase. Surface tension and electrostatic attraction between sweat residue and phosphor powder, resulting from frictional charges may also play an important role in the adhesion of the phosphor powder. As seen from Fig. 4, amino acids and esters present in human sweat react with each other in the presence of halide ions to form amides. The resulting amide product interacts with the as-synthesized LA phosphor *via* non-covalent electrostatic interactions. This phenomenon is attributed to a physical adsorption process also known as physisorption. Apart from the physical interaction, hydrophobic interactions of the  $\text{SrAl}_2\text{O}_4$  phosphor with the fingerprint residue can also strengthen the binding properties of the phosphor with the fingerprint residue.

Fig. 5 shows the room-temperature photoluminescence (PL) emission spectrum recorded in the range of 450–650 nm under visible light excitation (418 nm). The excitation spectra of the as-prepared phosphor exhibit a broad range of excitation starting

Table 2 Chemical composition of sweat secretions<sup>25</sup>

Secretory glands	Location	Inorganic constituents	Organic constituents
Eccrine glands	All over the body, but the only type of gland on the palms of the hands and soles of the feet	Chloride, metal ions, sulphate, phosphate, bicarbonates, ammonia, and water (>98%)	Amino acids, proteins, urea, uric acid, lactic acid, sugars, creatinine, and choline
Apocrine glands	In the groin and the armpits; associated with hair follicles	Water (>98%) and iron	Proteins, carbohydrates, and sterols
Sebaceous glands	All over the body; the highest concentration is on the forehead and on the back		Glycerides, fatty acids, wax esters, sterol esters, sterols, and squalene

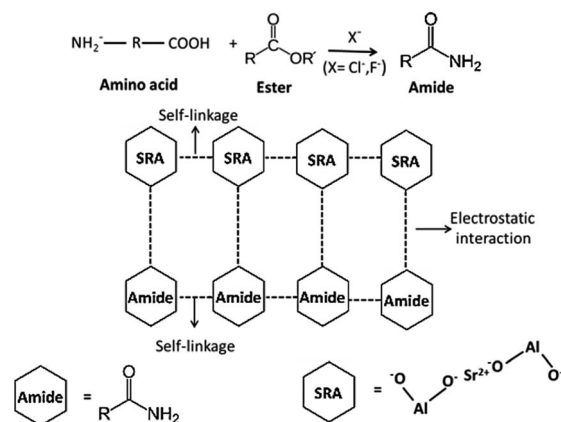


Fig. 4 Proposed mechanism involved in the physisorption process between the LA phosphor and sweat residue in fingerprints.

from near UV and extending to the visible range, *i.e.* from 280 nm to 470 nm. The broad excitation peak corresponds to the  $4f^7 \rightarrow 4f^65d^1$  transition of  $\text{Eu}^{2+}$  dopant ions. The excitation spectra are given in the ESI.†

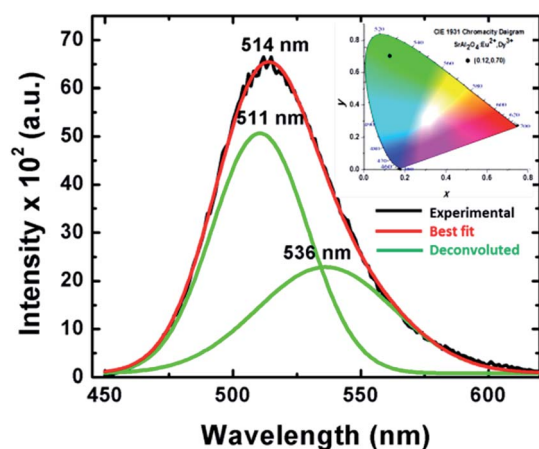


Fig. 5 Deconvoluted photoluminescence emission spectra of the  $\text{SrAl}_2\text{O}_4:\text{Eu}^{2+}, \text{Dy}^{3+}$  long afterglow phosphor recorded under visible light excitation. The red line is the sum of the fitting by Gaussian functions (green lines). The black solid line is the actual experimental data. The inset of the figure shows the CIE color coordinates of the green emitting  $\text{SrAl}_2\text{O}_4:\text{Eu}^{2+}, \text{Dy}^{3+}$  long afterglow phosphor.

The broad emission peak centered at 514 nm is the characteristic emission of parity allowed  $4f^65d^1 \rightarrow 4f^7$  transitions of  $\text{Eu}^{2+}$  ( $^8\text{S}_{7/2} \rightarrow ^2\text{D}_{5/2}$ ). The broad plateau-like absorption band is a consequence of the overlapping of two absorption bands from two europium sites substituted at two different crystallographic sites available for  $\text{Sr}^{2+}$  ions.<sup>27,28</sup>  $\text{Sr}^{2+}$  ions have two non-equivalent sites having different coordinations.  $\text{Eu}^{2+}$  ions can equally replace  $\text{Sr}^{2+}$  ions at two different coordinated sites resulting in a different degree of splitting of the  $4f^65d^1$  energy level since  $d \rightarrow f$  transitions are highly sensitive to local changes in the environment.<sup>29</sup> No characteristic emission from  $\text{Dy}^{3+}$  ions was observed from PL studies, which suggests that  $\text{Dy}^{3+}$  ions participate only as trapping centers. The inset presents the CIE color coordinates of the  $\text{SrAl}_2\text{O}_4:\text{Eu}^{2+}, \text{Dy}^{3+}$  phosphor calculated to be (0.12, 0.70) using the equidistant wavelength method. Also, the color purity of the PL emission has been estimated to be ~75%. Properties of bright fluorescence in the visible region, plus suitable particle size and shape, make LA phosphors an emerging class of materials ideal for latent fingerprinting applications in the fields of forensic and medical science.

Porous substrates are generally absorbent and fingerprint residues such as amino acids get absorbed into the substrate and do not migrate. Non-porous substrates do not absorb moisture and fingerprint residues are more susceptible to degradation since they reside on the outermost surface. In order to demonstrate the versatility of LA phosphors on various substrates we have used both porous black paper and non-porous polyterephthalate substrates. As mentioned earlier, developing high contrast latent fingerprints on highly colored backgrounds, using conventional contrasting powders, is difficult due to interference effects of the substrate.

The as-synthesized LA phosphor powder was dusted on fingerprints developed on transparent PET, non-porous substrates, light-colored PET substrates and porous black paper. Clear images of the developed fingerprints under UV (375 nm) were photographed as shown in Fig. 6. Also, images of fingerprints were shot in the dark after excitation, with the ambient light turned off. Fingerprints developed by using phosphor powder could be lifted by scotch tape and be preserved in evidence bags. The developed fingerprint marks could be re-excited as per the requirement.

As seen from Fig. 7, upon magnification, even the most minute details can be clearly appreciated in the developed

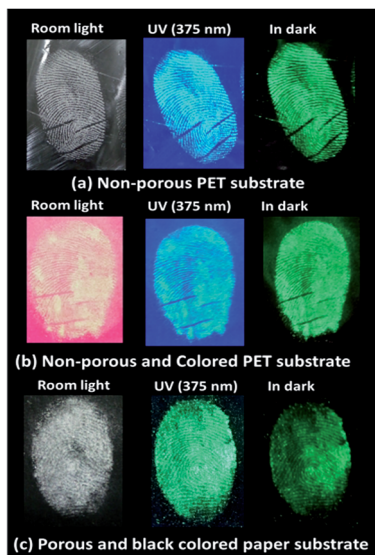


Fig. 6 (a) Luminescence images of the fingerprints produced on a transparent PET substrate, (b) colored PET substrate, and (c) porous black paper under white light and UV (375 nm), and afterglow images in the dark after excitation with white light for 5 minutes.

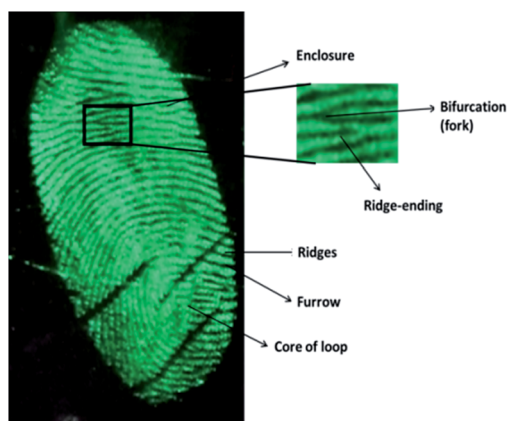


Fig. 7 Minute details in an as-developed fingerprint pattern in the dark upon magnification.

fingerprint and a suitable match will thus be easily and unequivocally determined. Both level 1 and level 2 fingerprint features can be clearly resolved. Level 1 features include ridge orientation and ridge pattern types. Level 2 features like short ridge, enclosure, bifurcation, and termination or combinations thereof can also be seen. These level 1 and level 2 features are used for classification, indexing, comparison and personal identification.

In conclusion, a novel application of an  $\text{SrAl}_2\text{O}_4:\text{Eu}^{2+}, \text{Dy}^{3+}$  long afterglow phosphor in extracting visually high contrast latent fingerprints from porous, non-porous, transparent and/or colored PET substrates is presented. Conventionally used fluorescent powders during crime scene investigations have limitations associated with interference of the background substrate with the fingerprints during lifting of the images. This

task becomes even more challenging if the images are to be extracted from transparent or colored PET substrates. The unusual property of visible light excitation of LA nanophosphors overcome the auto-fluorescence from the substrate resulting into high contrast fingerprint development without losing sensitive information due to ultraviolet irradiation and chemical processing by forensic experts. Compared to traditional fluorescent powders, LA phosphors offer several advantages of visible light excitation, negligible substrate interference, high contrast bifurcation of ridge patterns, and non-toxic nature, revealing finger ridge details of fingerprints.

## Conflicts of interest

There are no conflicts of interest to declare for this manuscript.

## Acknowledgements

We hereby declare that all experiments were performed in compliance with relevant laws or guidelines of our institute. Approval from the departmental research committee (DRC) has also been obtained before submitting the manuscript. As a part of the ethical policy, fresh fingermarks were collected from a healthy donor (G. Swati) aged 26 years, who is also one of the co-authors of this article with her prior written consent. GS and SB gratefully acknowledge the Council of Scientific and Industrial Research, Government of India under the Senior Research Fellowship schemes #31/1(448)/2015-EMR-1 and 31/1(445)/2015-EMR-1, respectively and Academy of Scientific and Innovative Research (AcSIR) for their support in carrying out the research work. DH and NL are grateful for the financial support from the Board of Research in Nuclear Sciences (BRNS), Government of India for the research project #34/14/16/2016-BRNS/34041.

## Notes and references

- 1 Y. Li, L. Xu and B. Su, *Chem. Commun.*, 2012, **48**, 4109–4111.
- 2 W. Song, Z. Mao, X. Liu, Y. Lu, Z. Li, B. Zhao and L. Lu, *Nanoscale*, 2012, **4**, 2333–2338.
- 3 H. C. Lee and R. E. Gaensslen, *Advances in Fingerprint Technology*, CRC Press, New York, 2001.
- 4 C. Champod, C. Lennard, P. Margot and M. Stoilovic, *Fingerprints and Other Ridge Skin Impressions*, CRC Press, Washington DC, 2004.
- 5 G. S. Sodhi and J. Kaur, *Egypt. J. Forensic Sci.*, 2016, **6**, 44.
- 6 A. Bécue, *Anal. Methods*, 2016, **8**, 7983.
- 7 G. Payne, B. Reedy, C. Lennard, B. Comber, D. Exline and C. Roux, *Forensic Sci. Int.*, 2005, **150**, 33.
- 8 B. J. Jones, A. J. Reynolds, M. Richardson and V. G. Sears, *Sci. Justice.*, 2010, **50**, 150.
- 9 M. Algarra, J. Jiménez-Jiménez, R. Moreno-Tost, B. B. Campos and J. C. G. Esteves da Silva, *Opt. Mater.*, 2011, **33**, 893.
- 10 J. Dilag, H. J. Kobus and A. V. Ellis, *Curr. Nanosci.*, 2011, **7**, 153.

- 11 M. Wang, M. Li, M. Yang, X. Zhang, A. Yu, Y. Zhu, P. Qiu and C. Mao, *Nano Res.*, 2015, **8**, 1800.
- 12 B.-Y. Li, X. L. Zhang, L. Y. Zhang, T. T. Wang, L. Li, C. G. Wang and Z. M. Su, *Dyes Pigm.*, 2016, **134**, 178.
- 13 H.-H. Xie, Q. Wen, H. Huang, T.-Y. Sun, P. Li, Y. Li, X.-F. Yu and Q.-Q. Wang, *RSC Adv.*, 2015, **5**, 79525.
- 14 W. He, T. S. Atabaev, H. K. Kim and Y. H. Hwang, *J. Phys. Chem. C*, 2013, **117**, 17894.
- 15 Y. Li, M. Gecevicius and J. Qiu, *Chem. Soc. Rev.*, 2009, **45**, 2090.
- 16 A. S. Paterson, B. Raja, G. Garvey, A. Kolhatkar, A. E. V. Hagström, K. Kourentzi, T. Randall Lee and R. C. Willson, *Anal. Chem.*, 2014, **86**, 9481.
- 17 I. P. Sahu, D. P. Bisen, N. Brahme and R. K. Tamraka, *J. Electron. Mater.*, 2016, **45**, 2222.
- 18 H. Sun, L. Pan, X. Piao and Z. Sun, *J. Colloid Interface Sci.*, 2014, **416**, 81.
- 19 I.-C. Kang, Q. Zhang, S. Yin, T. Sato and F. Saito, *Environ. Sci. Technol.*, 2008, **42**, 3622.
- 20 X. Xiong, X. Yuan, J. Song and G. Yin, *Appl. Spectrosc.*, 2016, **70**, 995.
- 21 V. Sharma, A. Das and V. Kumar, *Mater. Res. Express*, 2016, **3**, 015004.
- 22 L. Liu, Z. Zhang, L. Zhang and Y. Zhai, *Forensic Sci. Int.*, 2009, **183**, 45.
- 23 G. Swati, S. Chawla, S. Mishra, B. Rajesh, N. Vijayan, B. Sivaiah, A. Dhar and D. Haranath, *Appl. Surf. Sci.*, 2015, **333**, 178.
- 24 W. Jia, H. Yuan, L. Lu, H. Liu and W. M. Yen, *J. Lumin.*, 1998, **424**, 76.
- 25 C. Champod, C. Lennard, P. Margot and M. Stoilovic, *Fingerprints and Other Ridge Skin Impressions*, CRC Press, New York, 2004.
- 26 A. Arshad, M. A. Farrukh, S. Ali, M. K. Rahman and M. A. Tahir, *J. Forensic Sci.*, 2015, **60**, 1182.
- 27 D. Dutczak, T. Jüstel and C. Ronda, *Phys. Chem. Chem. Phys.*, 2015, **17**, 15236.
- 28 Y. Wang, Y. Gong, X. Xu and L. Yanqin, *J. Lumin.*, 2013, **133**, 25.
- 29 J. K. Park, M. A. Lim, K. J. Choi and C. H. Kim, *J. Mater. Sci.*, 2005, **40**, 2069.